

Article

Evaluating the Influence of Nitrogen Fertilizers and Biochar on *Brassica oleracea* L. var. *botrytis* by the Use of Fourier Transform Infrared (FTIR) Spectroscopy

Daniela Losacco^{1,2,*}, Claudia Campanale¹, Marina Tumolo^{1,2}, Valeria Ancona¹, Carmine Massarelli¹ and Vito Felice Uricchio¹

¹ National Council of Research-Water Research Institute, CNR-IRSA, 70132 Bari, Italy

² Department of Biology, University of Bari, 70126 Bari, Italy

* Correspondence: daniela.losacco@ba.irsa.cnr.it

Abstract: The exponential growth of the human population requires an increasing application of nitrogen (N) fertilizers, causing environmental pollution. Biochar (B) amended soil has been suggested as a sustainable agricultural practice to improve crop yield and mitigate agricultural pollutants' contamination. Evaluating the effect of fertilization on Brassica crops, in combination with spectral analysis, may specify changes in the chemical composition of the vegetable as a result of N fertilization. This study characterized cauliflower tissues treated with N fertilizer and biochar, employing Fourier Transform Infrared spectroscopy. The experiment was conducted in cauliflower mesocosms treated with two doses of N fertilizer (130 and 260 kg N ha⁻¹) with or without B. Attenuated total reflectance fractions were used to characterize fractions of curds, leaves, stems, and roots in the infrared using a Fourier transform. Principal component analysis was performed to classify the main differences among cauliflower tissues concerning treatments. FTIR spectra of *Brassica oleracea* L. var. *botrytis* tissues were related to nitrogen-based agricultural practices. The specific molecules associated with functional groups in cauliflower tissues were phenols, amides, proteins, amines, and glucosinolates. Biochar amended soil resulted in higher peaks that correspond to the stretching of phenols and proteins. The application of sustainable nitrogen fertilizers might influence the absorption bands characteristic of cauliflower's typical metabolites. The research allows the identification of Brassicaceae's functional molecules with a potential agronomic application.

Keywords: FTIR for spectral analysis; *Brassica oleracea* L. *botrytis*; biochar; nitrogen fertilization; sustainability; plant metabolites



Citation: Losacco, D.; Campanale, C.; Tumolo, M.; Ancona, V.; Massarelli, C.; Uricchio, V.F. Evaluating the Influence of Nitrogen Fertilizers and Biochar on *Brassica oleracea* L. var. *botrytis* by the Use of Fourier Transform Infrared (FTIR) Spectroscopy. *Sustainability* **2022**, *14*, 11985. <https://doi.org/10.3390/su141911985>

Academic Editor: Christophe Waterlot

Received: 17 August 2022

Accepted: 19 September 2022

Published: 22 September 2022

Publisher's Note: MDPI stays neutral with regard to jurisdictional claims in published maps and institutional affiliations.



Copyright: © 2022 by the authors. Licensee MDPI, Basel, Switzerland. This article is an open access article distributed under the terms and conditions of the Creative Commons Attribution (CC BY) license (<https://creativecommons.org/licenses/by/4.0/>).

1. Introduction

Vegetables are a fundamental food in human nutrition, providing essential dietary vitamins, minerals, carbohydrates, protein, and fiber [1], and also natural anti-cancer phytochemicals, known as glucosinolates [2]. Cauliflower (*Brassica oleracea* L. var. *botrytis*) is one of the essential varieties of *B. oleracea*, cultivated worldwide for its nutritional content [3].

Nitrogen (N) fertilizers are essential for the biosynthesis of plant metabolites and to ensure a strong crop yield, but usually, the application of agrochemicals takes place in higher quantities that the plants require [4–6]. Excess nitrogen is released into the soil through leaching, agricultural runoff, and/or air convections causing widespread and prolonged environmental contaminations [7]. Studies show that about 50% of N fertilizers are dispersed by volatilization and 5–10% by leaching phenomena [8].

Nitrogen losses cause various forms of environmental contamination in the air and surface-ground water bodies. Nitrate leaching determines the loss of groundwater quality [9] and the toxicity of drinking water [10].

New green strategies have been developed to control the release of agricultural nitrogenous pollutants and reduce the application of N fertilizers [11], such as organic waste [12–14].

Biochar is a carbonaceous material produced from the pyrolysis of biological waste—like wood, wastes of agricultural biomass, and manures—in the absence of oxygen at high temperatures [15]. Biochar-amended soil has been reported to improve soil quality and fertility, with a consequent increase in crop yield [11]. Biochar application in soil raises soil pH, improves cation exchange capacity, and retains nutrients [7,16–20]. In addition, recent studies highlight the benefits of biochar in climatic aspects [21–24], for the remediation of inorganic pollutants [25], soil amendment [26], wastewater treatment [27], and nutrient recovery [28]. Biochar can also be engineered to enhance adsorption [29]. However, the potential of biochar is widely dependent on the crop species and its type. It has been tested to enhance the Chinese cabbage biomass (*Brassica chinensis*) by 111–750%, depending on the quantity applied and the composition of the substrate [30]. Recent studies have proven the biochar capability of increasing *Brassica oleracea* L. yields, while at the same time avoiding the N and P leaching losses caused by nitrogen fertilization adopted by farmers. The biochar application resulted in mitigating the ammonium, and phosphorous leaching losses by 20–30% and 29–32%, respectively [31]. Another scientific work evaluated wood biochar on two genotypes of cabbage. The results proved that the mesoporous structures of the amended biochar (with its diverse functional groups) is a sustainable strategy that can increase growth and the efficiency of nitrogen use by regulating nitrogen-metabolizing enzymes, lowering tissue nitrate levels, and improving concentrations of minerals and the overall nutritional quality of cabbage [32]. However, the effect of biochar application in soils treated with N agrochemicals on chemical compounds in plant tissues of *Brassica oleracea* L. var. *botrytis* has not been studied at all.

In recent decades, new sensing technologies have been proposed in the agricultural field [33,34]. Specifically, attenuated total reflectance–Fourier transform infrared spectroscopy (ATR-FTIR) has been applied to examine the physicochemical property of soil treated by fertilizers and improvers [35–37], the crops biochemical composition [38], the agri-food quality [39,40], and the micro-organisms characterization [41]. In addition, ATR-FTIR has gained popularity among food and agriculture scientists as a promising non-destructive, and fast technique for detecting the molecular structure of various biopolymers, such as protein, carbohydrates, and lipids, in vegetables like Brassicaceae [42,43].

In particular, the first analyses in Brassicaceae were developed for *Brassica napus* and *Brassica rapa* [44], *Brassica carinata* and *Brassica juncea* using near-infrared reflectance spectroscopy [45]. Of course, the nutritional properties of Brassicaceae, both in content and type of metabolites, differ in response to agronomic factors [46].

In light of this, the main goal of this work was to characterize the chemical composition of different plant tissues of *Brassica oleracea* L. var. *botrytis* plants, in biochar-amended soils with different nitrogen doses, by attenuated total reflectance in the infrared with Fourier transform (ATR-FTIR).

2. Materials and Methods

2.1. Plant Material and Experimental Design

The study was performed in co-operation with ReAgri S.r.l. (Massafra, Taranto, Italy) between October 2020 and February 2021. The study was performed in a greenhouse over a natural photoperiod. *Brassica oleracea* L. var. *botrytis* seedlings (Akara, Syngenta) were transplanted into pots three weeks post sowing (three replicate pots per treatment). The pot size was 40 cm × 37 cm, and there were a total of fifteen pots in the experimental agronomic area. As shown in Figure 1, plants were covered with plastic sheeting to prevent the addition of rain.



Figure 1. Greenhouse experiment with three cauliflower plants per treatment. The plastic cloth was used to prevent the addition of rainwater.

The agricultural practice of synthetic nitrogen fertilization has provided (a) a standard application dose (130 kg N ha^{-1}), defined as normal dose (ND), and (b) a high application dose (260 kg N ha^{-1}), defined as high dose (HD) [47], in comparison with biochar-amended soils (ND+B and HD+B, respectively). Control plants were not fertilized (Figure 2). Calcium nitrate-based fertilizer (14.4% N) was applied to the soil layer between 0 and 30 cm [48]. In biochar-amended soils, 3% of the total volume of wood biochar was mixed with the soil, as recommended on the label (800–900 °C, Syngasmart, Rieti, Italy). The chemical properties of the biochar were: total N = 0.5%; total K = 0.4%; total P = 0.3%; total Ca = 1.1%; total Na = 0.2%; total Mg = 0.2%; organic carbon content = 68.40 mg/kg; pH = 11.3; electrical conductivity = 5.0 dS/m.

For the pot experiment, fertilizer application was divided into two phases [49]. In particular, the practice was carried out during the flowering induction phase (about 8 weeks after the transplantation stage) and the inflorescence enlargement phase (about 20 weeks after the transplantation stage). Biochar was amended with the 15 cm soil layer, before transplanting. The plants were harvested when the curds reached the market size.

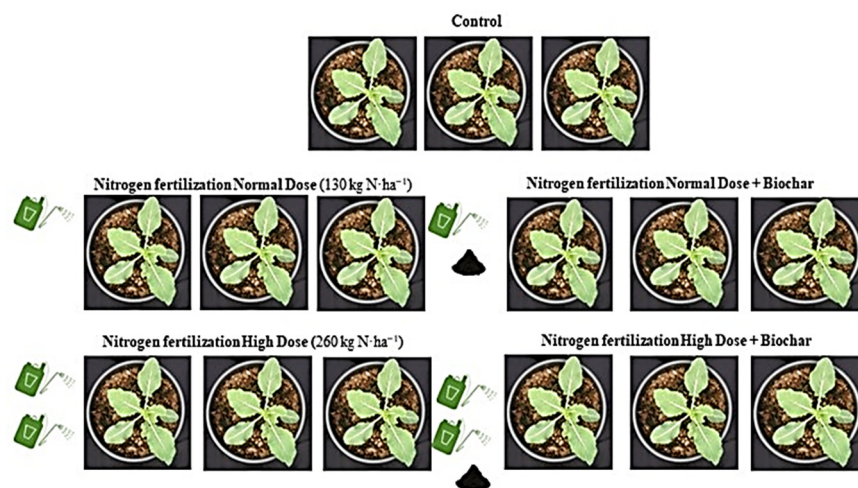


Figure 2. Agronomic design showing the five experimental lines.

2.2. Sample Preparation and Spectral Measurements

At the harvesting stage of the cauliflower curd, four vegetative tissues (roots, stems, leaves, and curds) were sampled for the analyses. The second leaf of each plant, starting from the curd, was collected for analysis. To avoid problems caused by humidity content on FTIR spectra, each fraction was dried in an oven at 60 °C. All fractions were the same

weight [50]. The samples were ground into powder in a mortar and characterized by ATR-FTIR using a Nicolet Summit FTIR Spectrometer (ThermoFisher Scientific, Waltham, MA, USA) equipped with an Everest ATR with a diamond crystal plate and a DTGS KBr detector. The IR absorption spectra of the samples were recorded from 4000 to 400 cm^{-1} with a spectral resolution of 4 cm^{-1} and 32 scans per sample [51]. The background was measured with the same settings against air. The sample spectra were obtained by spreading the sample on the surface of the crystal.

2.3. Data Analysis

The spectral data were examined using the OMNIC software (ThermoFisher, Waltham, MA, USA), which analyzed the entire region (3700–400 cm^{-1}). For spectral analysis, the OriginPro 8.5 program was utilized. The analysis was carried out by comparing the FTIR spectral peaks. To further classify the spectra and highlight the distribution of cauliflower tissues, the principal component analysis (PCA), a multivariate statistic method, was performed using the OriginPro 2022 software.

The principal component analysis provided qualitative information on the significant spectral components, where dominant variables determine the differences among the samples. The analysis is used to extract a small set of important principal components (PCs) of a correlation matrix that explain, easier than original data, the most variability of a dataset. The principal component analysis is constructive in its interpretation of FTIR spectra.

3. Results and Discussion

Fourier transform infrared spectroscopy (FTIR) is a technique used for the rapid, precise, and non-destructive characterization of marketable food compounds [49]. *Brassica oleracea* L. var. *botrytis* is a cruciferous that contains molecules and antioxidants such as glucosinolates, vitamins, flavonoids, phenolics, and sulforaphane. As shown in Figure 3, the FTIR spectra were acquired for each cauliflower tissue, corresponding to soil treated with a normal dose and a high dose of inorganic fertilizer (ND and HD, respectively), with and without biochar (ND+B and HD+B). All spectra presented similar profiles with different absorbances across the spectrum (Tables 1–4).

Table 1. Fourier transform infrared spectroscopy of cauliflower leaves from different treatments. The absorbance values are shown in brackets; n/d: band not detected.

Vibration	Wavenumber (cm^{-1})				
	C	ND	Treatments ND+B	HD	HD+B
O-H	3300 (0.39)	3264 (0.17)	3260 (0.19)	3270 (0.23)	3277 (0.22)
C-H	2919 (0.19)	2917 (0.23)	2918 (0.25)	2919 (0.28)	2917 (0.25)
C=O	1735 (0.14)	n/d	n/d	n/d	n/d
C=N	1606 (0.22)	1586 (0.28)	1587 (0.31)	1594 (0.35)	1598 (0.32)
N-O	n/d	n/d	n/d	n/d	n/d
C=N-O	1413 (0.21)	1401 (0.27)	1403 (0.3)	1405 (0.33)	1397 (0.33)
C-O	1242 (0.2)	1241 (0.22)	1241 (0.23)	1241 (0.26)	1241 (0.25)
S=O	1012 (0.45)	1016 (0.37)	1016 (0.41)	1009 (0.45)	1023 (0.39)

C—Control; ND—Normal Dose; ND+B—Normal Dose and Biochar; HD—High Dose; HD+B—High Dose and Biochar.

Table 2. Fourier transform infrared spectroscopy of cauliflower curds in different treatments. The absorbance values are shown in brackets; n/d: band not detected.

Vibration	Wavenumber (cm ⁻¹)				
	C	ND	Treatments ND+B	HD	HD+B
O-H	3278 (0.19)	3277 (0.22)	3279 (0.18)	3280 (0.18)	3276 (0.16)
C-H	2919 (0.18)	2922 (0.2)	2920 (0.18)	2919 (0.18)	2919 (0.16)
C=O	nd	nd	nd	nd	nd
C=N	1601 (0.21)	1621 (0.24)	1625 (0.22)	1617 (0.21)	1618 (0.17)
N-O	n/d	n/d	1535 (0.2)	n/d	n/d
C=N-O	1400 (0.21)	1402 (0.24)	1401 (0.2)	1376 (0.2)	1401 (0.17)
C-O	1238 (0.2)	1238 (0.22)	1233 (0.19)	1236 (0.19)	1236 (0.17)
S=O	1023 (0.34)	1016 (0.38)	1023 (0.26)	1027 (0.27)	1019 (0.22)

C—Control; ND—Normal Dose; ND+B—Normal Dose and Biochar; HD—High Dose; HD+B—High Dose and Biochar.

Table 3. Fourier transform infrared spectroscopy of cauliflower stems from different treatments. The absorbance values are shown in brackets; n/d: band not detected.

Vibration	Wavenumber (cm ⁻¹)				
	C	ND	Treatments ND+B	HD	HD+B
O-H	3285 (0.14)	3285 (0.15)	3293 (0.09)	3298 (0.08)	3321 (0.13)
C-H	2924 (0.14)	2920 (0.15)	2919 (0.08)	2920 (0.08)	2916 (0.11)
C=O	1735 (0.14)	n/d	n/d	1735 (0.07)	1735 (0.09)
C=N	1603 (0.15)	1604 (0.17)	1596 (0.09)	1597 (0.08)	1596 (0.13)
N-O	n/d	1508 (0.08)	1504 (0.08)	n/d	n/d
C=N-O	1370 (0.15)	1413 (0.18)	1408 (0.09)	1420 (0.08)	1413 (0.14)
C-O	1238 (0.16)	1231 (0.18)	1234 (0.09)	1233 (0.08)	1236 (0.14)
S=O	1018 (0.23)	1024 (0.27)	1025 (0.13)	1019 (0.12)	1022 (0.24)

C—Control; ND—Normal Dose; ND+B—Normal Dose and Biochar; HD—High Dose; HD+B—High Dose and Biochar.

Table 4. Fourier transform infrared spectroscopy of cauliflower roots from different treatments. The absorbance values are shown in brackets; n/d: band not detected.

Vibration	Wavenumber (cm ⁻¹)				
	C	ND	Treatments ND+B	HD	HD+B
O-H	3284 (0.03)	3283 (0.13)	3288 (0.16)	3285 (0.15)	3289 (0.19)
C-H	2918 (0.03)	2920 (0.11)	2920 (0.14)	2920 (0.14)	2920 (0.18)
C=O	1734 (0.22)	n/d	n/d	n/d	n/d
C=N	1604 (0.03)	1603 (0.15)	1604 (0.18)	1605 (0.16)	1566 (0.24)
N-O	n/d	n/d	n/d	n/d	n/d
C=N-O	1396 (0.03)	1410 (0.14)	1366 (0.19)	1365 (0.17)	1402 (0.25)
C-O	1234 (0.03)	1243 (0.13)	1235 (0.17)	1235 (0.16)	1235 (0.23)
S=O	1019 (0.08)	1019 (0.29)	1022 (0.3)	1019 (0.26)	1019 (0.41)

C—Control; ND—Normal Dose; ND+B—Normal Dose and Biochar; HD—High Dose; HD+B—High Dose and Biochar.

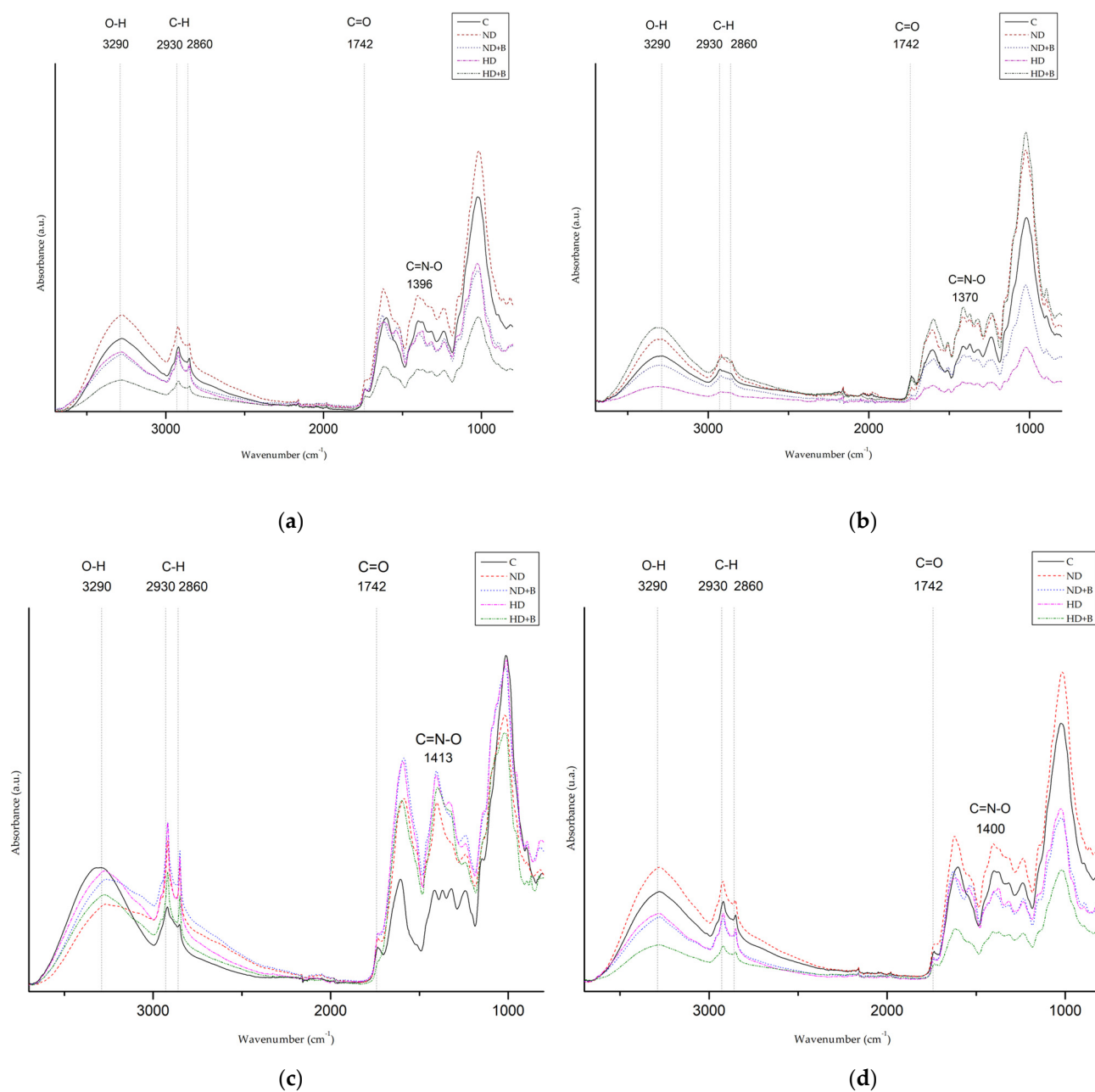


Figure 3. Infrared spectra with Fourier transform for different cauliflower plant tissues over the whole spectrum region: (a) roots; (b) stems; (c) leaves, and (d) curds. In legend: C—Control; ND—Normal Dose; ND+B—Normal Dose and Biochar; HD—High Dose; HD+B—High Dose and Biochar.

FTIR spectra comparison provided information on the four cauliflower tissues and their treatments (Figure 4). The overall spectra features are predominated by peaks corresponding to major functional groups and show comprehensive information on the sample's phenolics, compounds, proteins, and sulforaphane/glucosinolates [44,45].

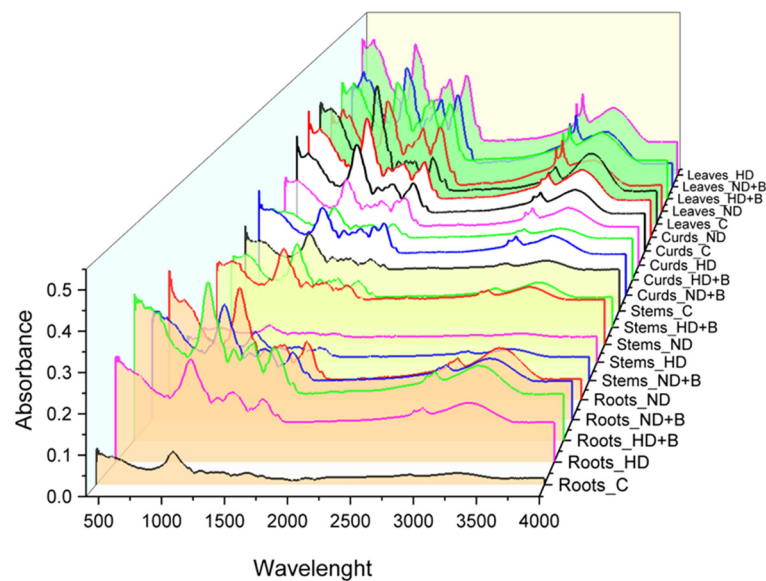


Figure 4. ATR-FTIR spectra obtained at 4000–500 cm^{-1} for all samples.

All samples showed characteristic peaks centered at 3290 cm^{-1} (assigned to O-H stretching of alcohols or phenols) and at 2930–2860 cm^{-1} (assigned to C-H stretching of alkynes). The peaks at 1742 cm^{-1} were associated to C=O, typical in carboxylic acids. The absorption at 1649 cm^{-1} and 1540 cm^{-1} was assigned to amide-stretching protein bands. The peak at 1400 cm^{-1} and a sharp peak at 1051 cm^{-1} , were also attributed to sulfones-stretching vibration in sulforaphane/glucosinolates. At the same time, the band at 1235 cm^{-1} (C=O) was assigned to the ester chain.

Biochar-amended soil caused changes in the absorbance of the cauliflower tissues, with differences observed in the region between 3200 and 2860 cm^{-1} , associated with bands typical of carboxylic acids (Figure 3) and to the existence of polysaccharides, lipids, and carbohydrates [52]. In the fingerprint region, between 1900 and 800 cm^{-1} , the main differences were highlighted with N doses of fertilizer and biochar application, corresponding to the presence of specific compounds associated with environmental stress [53] and, therefore, to the availability of nitrogenous nutrients. A significant difference in IR absorbance within the protein spectral region has also been demonstrated in the FTIR study of *B. carinata* [54].

As shown in Figure 4, using the green soil improver resulted in high absorbance values in the fingerprint region of both roots and cauliflower leaves, corresponding of principal compounds in the family of Brassicaceae [45].

The highest absorbance levels at $\sim 1051 \text{ cm}^{-1}$ were observed in the cauliflower leaves and the roots of plants treated with biochar (Figure 5a, Tables 1–4), probably due to the stability of the bond induced by the use of the carbonaceous material [55].

In the foliar tissues of plants that received a high nitrogen application dose, with and without biochar, high levels of absorbance relative to the peaks at ~ 1650 and $\sim 1400 \text{ cm}^{-1}$ of amide stretching (pink and green lines, Figure 5c; Table 1). In line with this study, Lu et al.'s [56] research on *Brassica napus* has also demonstrated the variability of protein levels with high levels of nitrogen fertilizers.

In contrast, the peak at $\sim 1000 \text{ cm}^{-1}$ characteristic of sulfones was high in the leaves of untreated cauliflower plants and fertilized with a standard application dose (black line, Figure 5c). Changes in the absorbance region between 1100–900 cm^{-1} were also observed by [57] under a lower N condition, demonstrating that these molecules are associated with the nitrogenous fertilization. The FTIR spectra comparison in the fingerprint region shows higher peaks relative to the main functional groups, characterizing absorbance in the fingerprint region of the curd were higher in the C and ND experimental lines, confirming

that many Brassicaceae compounds are related with sustainable nitrogen fertilization practices.

A reduction in absorbance was found for the functional group of sulfones (peaks at 1051 cm^{-1}) in cauliflower stems treated with a high dose of nitrogen fertilizer (HD) and in ND+B (blue and pink lines, respectively, Figure 5b; Table 3). High absorbance values at a wavelength of ~ 1600 and $\sim 1400\text{--}1051\text{ cm}^{-1}$ were highlighted in control plant curds fertilized with normal doses of calcium nitrate (Figure 5d), proving that the contents of organic molecules (protein, amines, and glucosinolates) were influenced by N doses.

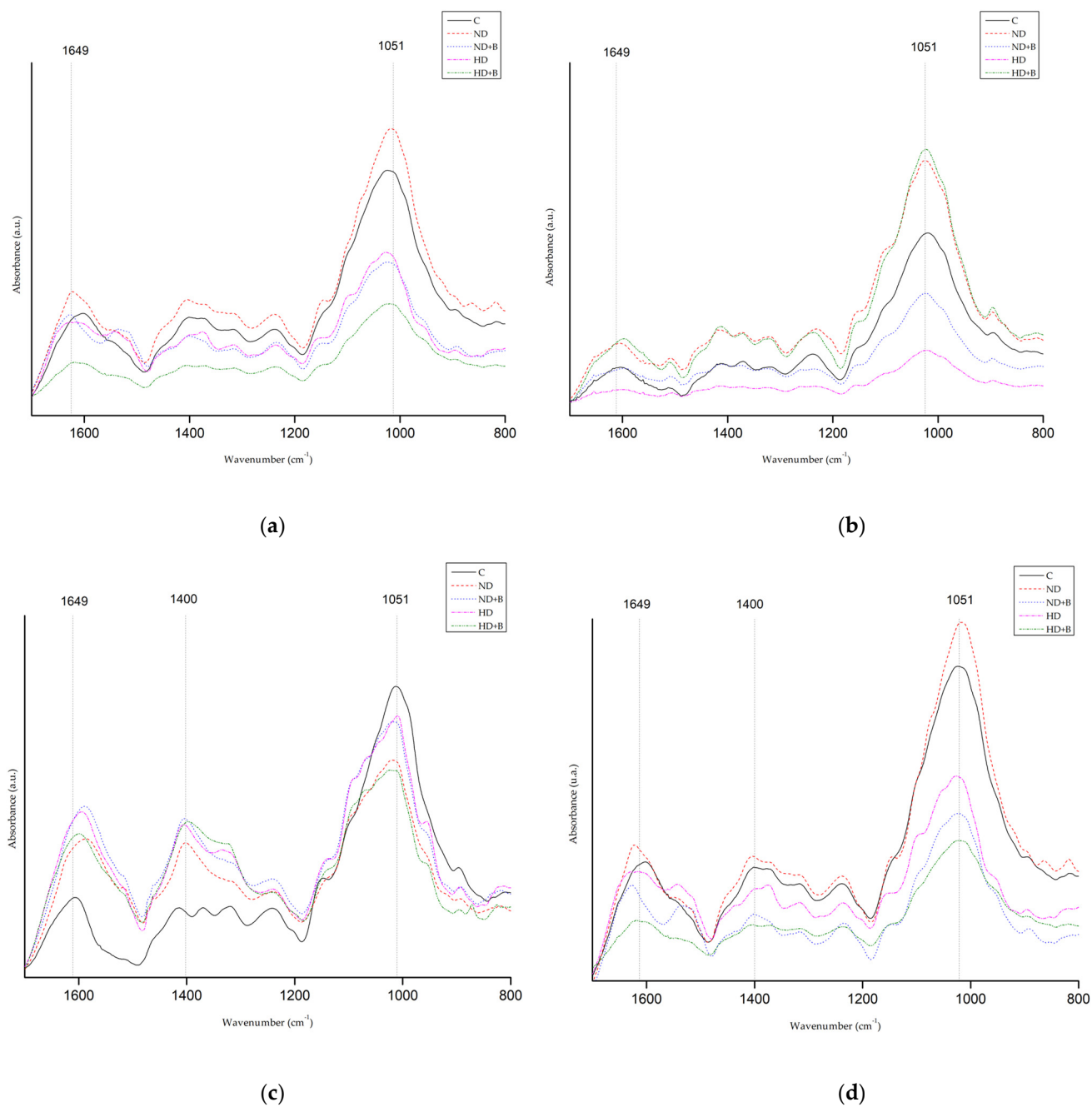


Figure 5. Infrared spectra with Fourier transform in the fingerprint region of cauliflower roots (a); stems (b); leaves (c) and curds (d).

The changes in absorbance were observed in several species treated with the different doses of nitrogen in the fertilizer [58–60], but the study of biochar’s influence on the content of cauliflower organic molecules has not been investigated.

The characteristic flavor of the curd is determined by the glucosinolate (GLS) content. The pattern of these molecules in individual plants is fixed early in life, perhaps as a response to early exposure to different environmental factors, such as salinity, drought, and nutritional deficiency [61]. An excessive amount of nitrogen may cause a decrease in total GLS, while a low amount of N produces an increase in total GLS when S supply is not limiting [62,63]. In addition, the transient allocation and distribution of glucosinolates modifies according to environmental changes [53].

In this research, the absorption values of each FTIR spectrum acquired in the range of 4000–400 cm^{-1} were utilized to perform the PCA. Table 5 exhibits variance that accounts for the first four principal components (PCs) computed from the absorbance value of the FTIR spectra of different vegetable tissues. The first three PCs outlined more data variance than any other PC and represented more than 99.27% of the data variation. The scores scatter plots PC1 (explained 89.7% of variability) \times PC2 (explained 7.8% of variability) were used to obtain separation of each group in the 1800–1200 cm^{-1} region.

Table 5. Variance distribution of the first four PCs of the vegetable tissues’ spectra.

Principal Component Number	Eigenvalue	Percentage of Variance (%)	Cumulative (%)
1	19.88754	89.71161	89.71161
2	1.67916	7.57461	97.28622
3	0.43998	1.98474	99.27096
4	0.06031	0.27206	99.54302

Figure 6 shows the score plot based on the first two PCs. The score plot indicates that the curds can be well separated in a separate ellipse, and in brief, the PCAs obtained on FTIR spectra discriminated samples mainly according to their chemical-physical properties, identifying well-distinguished groups based on the kind of vegetable tissue analyzed.

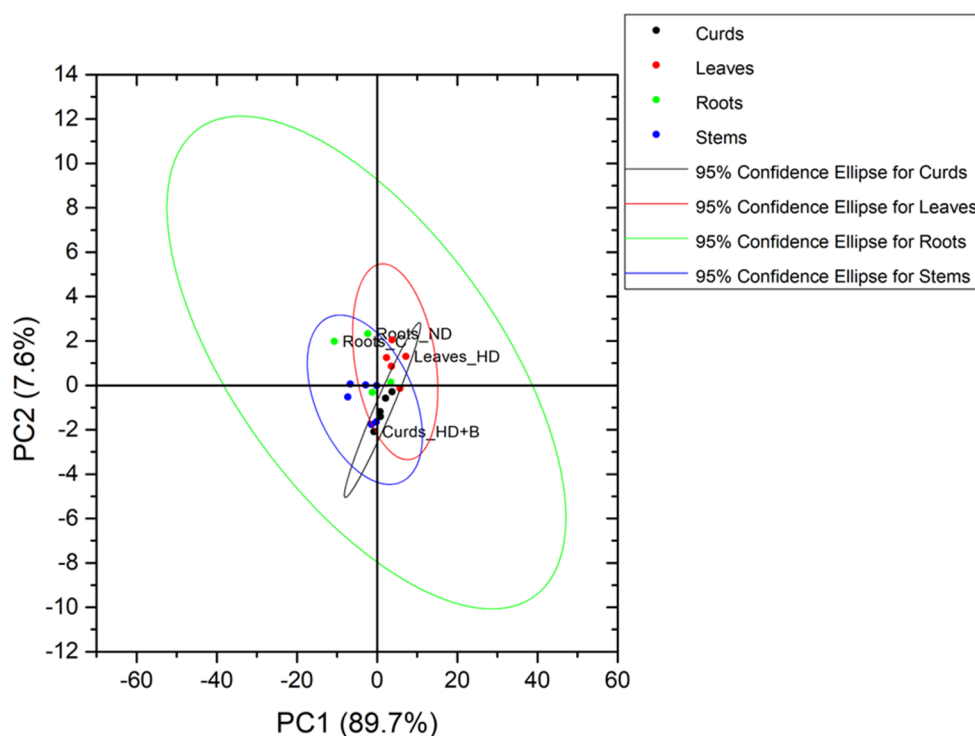


Figure 6. The plot of FTIR spectra of the four cauliflower tissues on PCA.

4. Conclusions

New sustainable agronomic practices include the application of green soil improvers, such as biochar, to enhance agricultural yield and the quality of environmental matrices. Specific organic molecules associated with functional groups characteristic of roots, stems, leaves, and inflorescences, are affected by the application of nitrogenous fertilizers, with the consequent change of the absorption peaks. Biochar application determines the increase in the number of phenolic compounds, carbohydrates, and proteins in cauliflower plants, in the presence of nitrogenous fertilizers. Low levels of N fertilizers increase the functional groups characteristic of glucosinolates, which are secondary metabolites of Brassicaceae with antioxidant activity.

This research identifies functional groups of *Brassica oleracea* L. var. *botrytis* with considerable importance in the nutraceutical and pharmacological fields. The protection afforded by the active ingredients in cauliflower is mainly attributed to their antioxidant activity and the presence of high amounts of GLS in the edible parts. Glucosinolates represent molecules devoid of toxicity and are easy to use as food integrators for maintaining a good state of health, reducing the risk of contracting degenerative diseases, such as tumors.

The results from this study demonstrate the potential of ATR-FTIR technology in studying changes in plant compounds in response to agricultural fertilization practices. Applying this new technology, together with the techniques of quantifying metabolites, will allow an improvement of the agricultural products on the market, respecting the environmental quality.

Author Contributions: Conceptualization, D.L., C.C., C.M., V.A. and V.F.U.; methodology, D.L., C.C. and M.T.; software, D.L. and C.C.; formal analysis, D.L., C.C. and M.T.; investigation D.L., C.M., V.A. and V.F.U.; data curation, D.L. and C.C.; writing—original draft preparation, D.L., C.C. and M.T.; writing—review and editing, D.L., C.C., M.T., V.A., C.M. and V.F.U.; supervision, V.A., C.M. and V.F.U.; project administration, D.L. and C.C.; funding acquisition, V.F.U. All authors have read and agreed to the published version of the manuscript.

Funding: This research was funded by project “Attuazione Direttiva 91/676/CEE relativa alla protezione delle acque dall’inquinamento provocato dai nitrati provenienti da fonti agricole-art. 92 del D.Lgs. 152/2006-revisione delle Zone Vulnerabili da Nitrati di origine agricola e aggiornamento del Programma D’Azione Nitrati-Convenzione tra Regione Puglia e CNR-IRSA di Bari del 27/11/2019”.

Institutional Review Board Statement: Not applicable.

Informed Consent Statement: Not applicable.

Data Availability Statement: The data presented in this study are available on request from the corresponding author.

Acknowledgments: The agronomic technical support provided by F. Acquasanta, P. Carmignano, S. Convertini, and F.Fedele of ReAgri S.r.l. is appreciated.

Conflicts of Interest: The authors declare no conflict of interest.

References

1. Pawar, R.; Barkule, S. Study on effect of integrated nutrient management on growth and yield of cauliflower (*Brassica oleracea* var. *botrytis* L.). *J. Appl. Nat. Sci.* **2017**, *9*, 520–525. [[CrossRef](#)]
2. Wang, J.; Gu, H.; Yu, H.; Zhao, Z.; Sheng, X.; Zhang, X. Genotypic variation of glucosinolates in broccoli (*Brassica oleracea* var. *italica*) florets from China. *Food Chem.* **2012**, *133*, 735–741. [[CrossRef](#)]
3. Li, H.; Liu, Q.; Zhang, Q.; Qin, E.; Jin, C.; Wang, Y.; Wu, M.; Shen, G.; Chen, C.; Song, W.; et al. Curd development associated gene (CDAG1) in cauliflower (*Brassica oleracea* L. var. *botrytis*) could result in enlarged organ size and increased biomass. *Plant Sci.* **2017**, *254*, 82–94. [[CrossRef](#)]
4. Tei, F.; De Neve, S.; de Haan, J.; Kristensen, H.L. Nitrogen management of vegetable crops. *Agric. Water Manag.* **2020**, *240*, 106316. [[CrossRef](#)]
5. DA, B.; GR, J.; GA, S. Amending greenroof soil with biochar to affect runoff water quantity and quality. *Environ. Pollut.* **2011**, *159*, 2111–2118. [[CrossRef](#)]

6. Morgado, R.G.; Loureiro, S.; González-Alcaraz, M.N. Changes in soil ecosystem structure and functions due to soil contamination. In *Soil Pollution: From Monitoring to Remediation*; Elsevier: Amsterdam, The Netherlands, 2017; pp. 59–87, ISBN 9780128498736.
7. Sashidhar, P.; Kochar, M.; Singh, B.; Gupta, M.; Cahill, D.; Adholeya, A.; Dubey, M. Biochar for delivery of agri-inputs: Current status and future perspectives. *Sci. Total Environ.* **2020**, *703*, 134892. [[CrossRef](#)] [[PubMed](#)]
8. Kookana, R.S.; Sarmah, A.K.; Van Zwieten, L.; Krull, E.; Singh, B. Biochar application to soil. agronomic and environmental benefits and unintended consequences. *Adv. Agron.* **2011**, *112*, 103–143. [[CrossRef](#)]
9. Teutscheroova, N.; Houška, J.; Navas, M.; Masaguer, A.; Benito, M.; Vazquez, E. Leaching of ammonium and nitrate from Acrisol and Calcisol amended with holm oak biochar: A column study. *Geoderma* **2018**, *323*, 136–145. [[CrossRef](#)]
10. Choudhury, A.T.M.A.; Kennedy, I.R. Nitrogen fertilizer losses from rice soils and control of environmental pollution problems. *Commun. Soil Sci. Plant Anal.* **2005**, *36*, 1625–1639. [[CrossRef](#)]
11. Losacco, D.; Ancona, V.; De Paola, D.; Tumolo, M.; Massarelli, C.; Gatto, A.; Uricchio, V.F. Development of ecological strategies for the recovery of the main nitrogen agricultural pollutants: A review on environmental sustainability in agroecosystems. *Sustainability* **2021**, *13*, 7163. [[CrossRef](#)]
12. Buecker, J.; Kloss, S.; Wimmer, B.; Rempt, F.; Zehetner, F.; Soja, G. Leachate Composition of Temperate Agricultural Soils in Response to Biochar Application. *Water Air Soil Pollut.* **2016**, *227*, 49. [[CrossRef](#)]
13. Yoo, G.; Kim, H.; Chen, J.; Kim, Y. Effects of Biochar Addition on Nitrogen Leaching and Soil Structure following Fertilizer Application to Rice Paddy Soil. *Soil Sci. Soc. Am. J.* **2014**, *78*, 852–860. [[CrossRef](#)]
14. Sorrenti, G.; Toselli, M. Soil leaching as affected by the amendment with biochar and compost. *Agric. Ecosyst. Environ.* **2016**, *226*, 56–64. [[CrossRef](#)]
15. Singh, R.; Babu, J.N.; Kumar, R.; Srivastava, P.; Singh, P.; Raghubanshi, A.S. Multifaceted application of crop residue biochar as a tool for sustainable agriculture: An ecological perspective. *Ecol. Eng.* **2015**, *77*, 324–347. [[CrossRef](#)]
16. Altland, J.E.; Locke, J.C. Biochar Affects Macronutrient Leaching from a Soilless Substrate. *HortScience* **2012**, *47*, 1136–1140. [[CrossRef](#)]
17. Haque, M.M.; Rahman, M.M.; Morshed, M.M.; Islam, M.S.; Afrad, M.S.I. Biochar on Soil Fertility and Crop Productivity. *Agriculturists* **2019**, *17*, 76–88. [[CrossRef](#)]
18. Kammann, C.I.; Schmidt, H.P.; Messerschmidt, N.; Linsel, S.; Steffens, D.; Müller, C.; Koyro, H.W.; Conte, P.; Stephen, J. Plant growth improvement mediated by nitrate capture in co-composted biochar. *Sci. Rep.* **2015**, *5*, 11080. [[CrossRef](#)]
19. Prodana, M.; Bastos, A.C.; Silva, A.R.R.; Morgado, R.G.; Frankenbach, S.; Serôdio, J.; Soares, A.M.V.M.; Loureiro, S. Soil functional assessment under biochar, organic amendments and fertilizers applications in small-scale terrestrial ecosystem models. *Appl. Soil Ecol.* **2021**, *168*, 104157. [[CrossRef](#)]
20. Schulz, H.; Dunst, G.; Glaser, B. Positive effects of composted biochar on plant growth and soil fertility. *Agron. Sustain. Dev.* **2013**, *33*, 817–827. [[CrossRef](#)]
21. Lorenz, K.; Lal, R. Biochar application to soil for climate change mitigation by soil organic carbon sequestration. *J. Plant Nutr. Soil Sci.* **2014**, *177*, 651–670. [[CrossRef](#)]
22. Lehmann, J.; Cowie, A.; Masiello, C.A.; Kammann, C.; Woolf, D.; Amonette, J.E.; Cayuela, M.L.; Camps-Arbestain, M.; Whitman, T. Biochar in climate change mitigation. *Nat. Geosci.* **2021**, *14*, 883–892. [[CrossRef](#)]
23. Woolf, D.; Amonette, J.E.; Street-Perrott, F.A.; Lehmann, J.; Joseph, S. Sustainable biochar to mitigate global climate change. *Nat. Commun.* **2010**, *1*, 56. [[CrossRef](#)]
24. Qambrani, N.A.; Rahman, M.M.; Won, S.; Shim, S.; Ra, C. Biochar properties and eco-friendly applications for climate change mitigation, waste management, and wastewater treatment: A review. *Renew. Sustain. Energy Rev.* **2017**, *79*, 255–273. [[CrossRef](#)]
25. Zhang, X.; Wang, H.; He, L.; Lu, K.; Sarmah, A.; Li, J.; Bolan, N.S.; Pei, J.; Huang, H. Using biochar for remediation of soils contaminated with heavy metals and organic pollutants. *Environ. Sci. Pollut. Res.* **2013**, *20*, 8472–8483. [[CrossRef](#)]
26. Rajapaksha, A.U.; Chen, S.S.; Tsang, D.C.W.; Zhang, M.; Vithanage, M.; Mandal, S.; Gao, B.; Bolan, N.S.; Ok, Y.S. Engineered/designer biochar for contaminant removal/immobilization from soil and water: Potential and implication of biochar modification. *Chemosphere* **2016**, *148*, 276–291. [[CrossRef](#)]
27. Liu, P.; Liu, W.J.; Jiang, H.; Chen, J.J.; Li, W.W.; Yu, H.Q. Modification of bio-char derived from fast pyrolysis of biomass and its application in removal of tetracycline from aqueous solution. *Bioresour. Technol.* **2012**, *121*, 235–240. [[CrossRef](#)] [[PubMed](#)]
28. Li, R.; Wang, J.J.; Zhang, Z.; Awasthi, M.K.; Du, D.; Dang, P.; Huang, Q.; Zhang, Y.; Wang, L. Recovery of phosphate and dissolved organic matter from aqueous solution using a novel CaO-MgO hybrid carbon composite and its feasibility in phosphorus recycling. *Sci. Total Environ.* **2018**, *642*, 526–536. [[CrossRef](#)] [[PubMed](#)]
29. Li, R.; Deng, H.; Zhang, X.; Wang, J.J.; Awasthi, M.K.; Wang, Q.; Xiao, R.; Zhou, B.; Du, J.; Zhang, Z. High-efficiency removal of Pb(II) and humate by a CeO₂-MoS₂ hybrid magnetic biochar. *Bioresour. Technol.* **2019**, *273*, 335–340. [[CrossRef](#)] [[PubMed](#)]
30. Da Silva Leite, R.; Hernández-Navarro, S.; do Nascimento, M.N.; Potosme, N.M.R.; Carrión-Prieto, P.; dos Santos Souza, E. Nitrogen fertilization affects Fourier Transform Infrared spectra (FTIR) in *Physalis L.* species. *Comput. Electron. Agric.* **2018**, *150*, 411–417. [[CrossRef](#)]
31. Sun, H.; Jeyakumar, P.; Xiao, H.; Li, X.; Liu, J.; Yu, M.; Bir Jung Rana, P.; Shi, W. Biochar can Increase Chinese Cabbage (*Brassica oleracea L.*) Yield, Decrease Nitrogen and Phosphorus Leaching Losses in Intensive Vegetable Soil. *Phyton* **2022**, *91*, 197–206. [[CrossRef](#)]

32. Saffeullah, P.; Nabi, N.; Zaman, M.B.; Liaqat, S.; Siddiqi, T.O.; Umar, S. Efficacy of Characterized Prosopis Wood Biochar Amendments in Improving Growth, Nitrogen Use Efficiency, Nitrate Accumulation, and Mineral Content in Cabbage Genotypes. *J. Soil Sci. Plant Nutr.* **2021**, *21*, 690–708. [[CrossRef](#)]
33. Wu, K.; Du, C.; Ma, F.; Shen, Y.; Liang, D.; Zhou, J. Rapid diagnosis of nitrogen status in rice based on Fourier transform infrared photoacoustic spectroscopy (FTIR-PAS). *Plant Methods* **2019**, *15*, 94. [[CrossRef](#)] [[PubMed](#)]
34. Tarpley, L.; Reddy, K.R.; Sassenrath-Cole, G.F. Reflectance indices with precision and accuracy in predicting cotton leaf nitrogen concentration. *Crop Sci.* **2000**, *40*, 1814–1819. [[CrossRef](#)]
35. Cole, E.J.; Zandvakili, O.R.; Xing, B.; Hashemi, M.; Herbert, S.; Mashayekhi, H.H. Dataset on the effect of hardwood biochar on soil gravimetric moisture content and nitrate dynamics at different soil depths with FTIR analysis of fresh and aged biochar. *Data Br.* **2019**, *25*, 104073. [[CrossRef](#)] [[PubMed](#)]
36. Vamvuka, D.; Raftogianni, A. Evaluation of pig manure for environmental or agricultural applications through gasification and soil leaching experiments. *Appl. Sci.* **2021**, *11*, 12011. [[CrossRef](#)]
37. Liu, X.; Liao, J.; Song, H.; Yang, Y.; Guan, C.; Zhang, Z. A Biochar-Based Route for Environmentally Friendly Controlled Release of Nitrogen: Urea-Loaded Biochar and Bentonite Composite. *Sci. Rep.* **2019**, *9*, 9548. [[CrossRef](#)]
38. Ertani, A.; Francioso, O.; Ferrari, E.; Schiavon, M.; Nardi, S. Spectroscopic-chemical fingerprint and biostimulant activity of a protein-based product in solid form. *Molecules* **2018**, *23*, 1031. [[CrossRef](#)]
39. Wang, W.; Paliwal, A.J. Near-infrared spectroscopy and imaging in food quality and safety. *Sens. Instrum. Food Qual. Saf.* **2007**, *1*, 193–207. [[CrossRef](#)]
40. Cozzolino, D. Recent Trends on the Use of Infrared Spectroscopy to Trace and Authenticate Natural and Agricultural Food Products. *Appl. Spectrosc. Rev.* **2012**, *47*, 518–530. [[CrossRef](#)]
41. Barboux, R.; Bousta, F.; Di Martino, P. Ftir spectroscopy for identification and intra-species characterization of serpula lacrymans. *Appl. Sci.* **2021**, *11*, 8463. [[CrossRef](#)]
42. Gomaa, W.M.S.; Feng, X.; Zhang, H.; Zhang, X.; Zhang, W.; Yan, X.; Peng, Q.; Yu, P. Application of advanced molecular spectroscopy and modern evaluation techniques in canola molecular structure and nutrition property research. *Crit. Rev. Food Sci. Nutr.* **2020**, *61*, 3256–3266. [[CrossRef](#)] [[PubMed](#)]
43. Xin, H.; Khan, N.A.; Falk, K.C.; Yu, P. Mid-Infrared Spectral Characteristics of Lipid Molecular Structures in Brassica carinata Seeds: Relationship to Oil Content, Fatty Acid and Glucosinolate Profiles, Polyphenols, and Condensed Tannins. *J. Agric. Food Chem.* **2014**, *62*, 7977–7988. [[CrossRef](#)] [[PubMed](#)]
44. Vicas, S.I.; Cavalu, S.; Laslo, V.; Tocai, M.; Costea, T.O.; Moldovan, L. Growth, photosynthetic pigments, phenolic, glucosinolates content and antioxidant capacity of broccoli sprouts in response to nanoselenium particles supply. *Not. Bot. Horti Agrobot. Cluj-Napoca* **2019**, *47*, 821–828. [[CrossRef](#)]
45. Singh, A.; Sharma, B.; Deswal, R. Green silver nanoparticles from novel Brassicaceae cultivars with enhanced antimicrobial potential than earlier reported Brassicaceae members. *J. Trace Elem. Med. Biol.* **2018**, *47*, 1–11. [[CrossRef](#)] [[PubMed](#)]
46. Francisco, M.; Moreno, D.A.; Cartea, M.E.; Ferreres, F.; García-Viguera, C.; Velasco, P. Simultaneous identification of glucosinolates and phenolic compounds in a representative collection of vegetable *Brassica rapa*. *J. Chromatogr. A* **2009**, *1216*, 6611–6619. [[CrossRef](#)] [[PubMed](#)]
47. Di Gioia, F.; Santamaria, P. *Cavolfiore, Cavolo Broccolo e Cima di Rapa*; Santamaria, P., Serio, F., Eds.; CRSA: Locorotondo, Italy, 2009.
48. Jagadamma, S.; Lal, R.; Hoefl, R.G.; Nafziger, E.D.; Adee, E.A. Nitrogen fertilization and cropping systems effects on soil organic carbon and total nitrogen pools under chisel-plow tillage in Illinois. *Soil Tillage Res.* **2007**, *95*, 348–356. [[CrossRef](#)]
49. Losacco, D.; Tumolo, M.; Cotugno, P.; Leone, N.; Massarelli, C.; Convertini, S.; Tursi, A.; Uricchio, V.F.; Ancona, V. Use of Biochar to Improve the Sustainable Crop Production of Cauliflower (*Brassica oleracea* L.). *Plants* **2022**, *11*, 1182. [[CrossRef](#)]
50. Cruz, J.L.; Souza Filho, L.F.S.; Pelacani, C.R. Influência da adubação fosfatada sobre o crescimento do camapu (*Physalis angulata* L.). *Rev. Bras. Plantas Med.* **2015**, *17*, 360–366. [[CrossRef](#)]
51. Carrión-Prieto, P.; Hernández-Navarro, S.; Martín-Ramos, P.; Sánchez-Sastre, L.F.; Garrido-Lauraga, F.; Marcos-Robles, J.L.; Martín-Gil, J. Mediterranean shrublands as carbon sinks for climate change mitigation: New root-to-shoot ratios. *Carbon Manag.* **2017**, *8*, 67–77. [[CrossRef](#)]
52. Cao, Z.; Wang, Z.; Shang, Z.; Zhao, J. Classification and identification of Rhodobryum roseum Limpr. and its adulterants based on fourier-transform infrared spectroscopy (FTIR) and chemometrics. *PLoS ONE* **2017**, *12*, e0172359. [[CrossRef](#)]
53. Del Carmen Martínez-Ballesta, M.; Moreno, D.A.; Carvajal, M. The Physiological Importance of Glucosinolates on Plant Response to Abiotic Stress in Brassica. *Int. J. Mol. Sci.* **2013**, *14*, 11607. [[CrossRef](#)] [[PubMed](#)]
54. Xin, H.; Falk, K.C.; Yu, P. Studies on brassica carinata seed. 1. protein molecular structure in relation to protein nutritive values and metabolic characteristics. *J. Agric. Food Chem.* **2013**, *61*, 10118–10126. [[CrossRef](#)] [[PubMed](#)]
55. Zolfi Bavariani, M.; Ronaghi, A.; Ghasemi, R. Influence of Pyrolysis Temperatures on FTIR Analysis, Nutrient Bioavailability, and Agricultural use of Poultry Manure Biochars. *Soil Sci. Plant Anal.* **2019**, *50*, 402–411. [[CrossRef](#)]
56. Lu, Y.; Du, C.; Yu, C.; Zhou, J. Use of FTIR-PAS combined with chemometrics to quantify nutritional information in rapeseeds (*Brassica napus*). *J. Plant Nutr. Soil Sci.* **2014**, *177*, 927–933. [[CrossRef](#)]
57. Rubio-Díaz, S.; Pérez-Pérez, J.M.; González-Bayón, R.; Muñoz-Viana, R.; Borrega, N.; Mouille, G.; Hernández-Romero, D.; Robles, P.; Höfte, H.; Ponce, M.R.; et al. Cell Expansion-Mediated Organ Growth Is Affected by Mutations in Three EXIGUA Genes. *PLoS ONE* **2012**, *7*, e36500. [[CrossRef](#)] [[PubMed](#)]

58. Medina-Medrano, J.R.; Almaraz-Abarca, N.; Socorro González-Elizondo, M.; Uribe-Soto, J.N.; González-Valdez, L.S.; Herrera-Arrieta, Y. Phenolic constituents and antioxidant properties of five wild species of *Physalis* (Solanaceae). *Bot. Stud.* **2015**, *56*, 24. [[CrossRef](#)] [[PubMed](#)]
59. Bertocelli, D.J.; de Oliveira, M.C.; de Oliveira Bolina, C.; dos Passos, A.I.; Ariati, A.C.; Osmar, O.A. Chemical characteristics of fruits of two species of *Physalis* under nitrogen fertilization. *African J. Agric. Res.* **2016**, *11*, 1872–1878. [[CrossRef](#)]
60. Cobaleda-Velasco, M.; Alanis-Bañuelos, R.E.; Almaraz-Abarca, N.; Rojas-López, M.; González-Valdez, L.S.; Ávila-Reyes, J.A.; Rodrigo, S. Phenolic profiles and antioxidant properties of *Physalis angulata* L. as quality indicators. *J. Pharm. Pharmacogn. Res.* **2017**, *5*, 114–128.
61. Crisp, P.; Tapsell, C.R. Cauliflower. *Genet. Improv. Veg. Crop.* **1993**, 157–178. [[CrossRef](#)]
62. Schonhof, I.; Blankenburg, D.; Müller, S.; Krumbein, A. Sulfur and nitrogen supply influence growth, product appearance, and glucosinolate concentration of broccoli. *J. Plant Nutr. Soil Sci.* **2007**, *170*, 65–72. [[CrossRef](#)]
63. Velasco, P.; Cartea, M.E.; González, C.; Vilar, M.; Ordás, A. Factors affecting the glucosinolate content of kale (*Brassica oleracea* acephala group). *J. Agric. Food Chem.* **2007**, *55*, 955–962. [[CrossRef](#)]